# Intrinsic Depot-Specific Differences in the Secretome of Adipose Tissue, Preadipocytes, and Adipose Tissue–Derived Microvascular Endothelial Cells

**Samantha L. Hocking,[1] Lindsay E. Wu,[1,2] Michael Guilhaus,[2,†] Donald J. Chisholm,[1] and David E. James[1]**



**OBJECTIVE**—Visceral adipose tissue (VAT) is more closely linked to insulin resistance than subcutaneous adipose tissue (SAT). We conducted a quantitative analysis of the secretomes of VAT and SAT to identify differences in adipokine secretion that account for the adverse metabolic consequences of VAT.

**RESEARCH DESIGN AND METHODS**—We used lectin affinity chromatography followed by comparison of isotope-labeled amino acid incorporation rates to quantitate relative differences in the secretomes of VAT and SAT explants. Because adipose tissue is composed of multiple cell types, which may contribute to depot-specific differences in secretion, we isolated preadipocytes and microvascular endothelial cells (MVECs) and compared their secretomes to those from whole adipose tissue.

**RESULTS**—Although there were no discrete depot-specific differences in the secretomes from whole adipose tissue, preadipocytes, or MVECS, VAT exhibited an overall higher level of protein secretion than SAT. More proteins were secreted in twofold greater abundance from VAT explants compared with SAT explants (59% versus 21%), preadipocytes (68% versus 0%), and MVECs (62% versus 15%). The number of proteins in the whole adipose tissue secretome was greater than the sum of its cellular constituents. Finally, almost 50% of the adipose tissue secretome was composed of factors with a role in angiogenesis.

**CONCLUSIONS**—VAT has a higher secretory capacity than SAT, and this difference is an intrinsic feature of its cellular components. In view of the number of angiogenic factors in the adipose tissue secretome, we propose that VAT represents a more readily expandable tissue depot. ***Diabetes*** **59:3008–3016, 2010**

Obesity increases the risk of type 2 diabetes; however, the distribution of body fat may be more important than obesity per se (1). Visceral adiposity is associated with an increased risk of insulin resistance (2–4), and this relationship persists even in nonobese individuals (1). Similarly in rodents, increased adiposity in epididymal, mesenteric, and perinephric depots induces insulin resistance (5). There are several differences between visceral (VAT) and subcutaneous adipose tissue (SAT) that could account for the link between VAT and insulin resistance, the most obvious being anatomical location. VAT is particularly sensitive to lipolytic stimuli and partly drains into the liver via the portal vein. Increased flux of free fatty acids from VAT to liver may increase hepatic gluconeogenesis and hepatic insulin resistance (6,7). Data in both humans and rodents argue against this "portal hypothesis." Removal of gonadal (nonportal) adipose tissue in obese mice improves insulin sensitivity (8). In humans, some studies show a stronger association between subcutaneous abdominal fat and insulin resistance (9,10). Thus, the role of anatomical location in mediating the deleterious effects of VAT remains unresolved.

These divergent metabolic effects may be due to intrinsic, cell-autonomous differences between VAT and SAT. VAT displays higher rates of fatty acid uptake and release with reduced antilipolytic response to insulin (11), increased lipolytic response to catecholamines (12), increased response to glucocorticoids with increased lipoprotein lipase activation (13), and higher glucocorticoid receptor levels (14). Studies of gene expression have found major differences between adipocytes and preadipocytes from VAT and SAT (15). These data suggest intrinsic differences between cells in VAT and SAT.

Adipose tissue is an endocrine organ secreting numerous proteins (adipokines) with potent metabolic effects (16). Metabolically beneficial adipokines including leptin and adiponectin are secreted in higher amounts from SAT (17,18), whereas proinflammatory adipokines such as RBP4, TNF-α, MCP-1, IL-8, and IL-6 are increased in VAT (19–23). It has been suggested that this differential secretion of adipokines may account for the differing metabolic consequences of visceral and subcutaneous adiposity. However, it is unclear if these factors are secreted from adipocytes or other cells resident in adipose tissue such as macrophages. Whereas leptin and adiponectin are secreted by adipocytes, other factors including resistin, visfatin, TNF-α, IL-6, and MCP-1 are principally secreted by macrophages (24). Therefore, the adipocyte may not be the principal secretory component of adipose tissue.

We sought to accurately characterize the secretome of adipose tissue and quantitatively compare the secretomes from VAT and SAT explants. Previous studies identified adipocyte secretory factors using 3T3-L1 cell-lines (25,26) or primary adipocytes (27,28). These studies have several limitations. Immortalized cell lines are unable to provide depot specificity, and by isolating adipocytes from nonadipose cells within adipose tissue, cross-talk between these cells is lost. Using whole adipose tissue explants

From the [1]Diabetes and Obesity Program, Garvan Institute of Medical Research, Darlinghurst, NSW, Australia; and the [2]Bioanalytical Mass Spectrometry Facility, University of New South Wales, Sydney, NSW, Australia.
Corresponding author: David E. James, d.james@garvan.org.au.
Received 7 April 2010 and accepted 31 August 2010. Published ahead of print at http://diabetes.diabetesjournals.org on 14 September 2010. DOI: 10.2337/db10-0483.
S.L.H. and L.E.W. contributed equally to this study.
†Deceased.

avoids these issues but introduces the presence of non-adipose-derived contaminating serum proteins. To circumvent this problem, we used comparison of isotope-labeled amino acid incorporation rates (CILAIR) (29). Cells or tissues are incubated with isotopically labeled amino acids, which become incorporated into newly synthesized proteins. This method allows quantitative assessment of differences in protein secretion as a protein with a higher incorporation of isotope is synthesized at a greater rate or in greater abundance.

The quality of the secretome sample can also be diminished by contamination with cytosolic, nonsecretory proteins released from damaged cells. Secreted proteins commonly undergo N-glycosylation, whereas cytosolic proteins do not. We exploited differential N-glycosylation, using lectin affinity chromatography (LAC) to selectively enrich proteins targeted for secretion.

We used LAC followed by CILAIR (LAC-CILAIR) to quantitate relative differences in the secretomes of murine VAT and SAT. Because adipose tissue is composed of multiple cell types, which may contribute to depot-specific differences in secretion, we isolated preadipocytes and microvascular endothelial cells (MVECs) and compared their secretomes to that from whole adipose tissue. Although we did not observe any discrete differences in secretion profile between each depot, VAT exhibited an overall higher level of protein secretion than SAT, for whole adipose tissue, preadipocytes, and MVECS. Interestingly, a large proportion of the adipose tissue secretome was factors that play a role in angiogenesis. The increased production of these factors from VAT leads to the inescapable speculation that VAT represents a more readily expandable adipose tissue depot than SAT.

## RESEARCH DESIGN AND METHODS

**Materials and buffers.** All tissue culture reagents were from Life Technologies unless otherwise stated.

**Transfer medium.** Dulbecco's modified eagle medium (DMEM)/Ham's F-12 1:1 containing 1% BSA and supplemented with 100 units/ml penicillin, 0.1 mg/ml streptomycin, and 0.25 μg/ml amphotericin B (antibiotic–antimycotic, Invitrogen).

**SILAC medium.** Low-glucose DMEM without leucine, lysine, and arginine (Sigma Aldrich) was supplemented with 0.105 g/l leucine, 100 units/ml penicillin, 0.1 mg/ml streptomycin, 0.0159 g/l phenol red, and 100 nmol/l insulin (DMEM/K-/R-). Glucose was added to a final concentration of 4.5 g/l. "Heavy" or "medium" isotopes of arginine (Cambridge Laboratories U-$^{13}$C6 units–$^{15}$N4 arginine CNLM-539 or U-$^{13}$C6 arginine CLM-2265 0.021 g/l) and lysine (Cambridge Laboratories U-$^{13}$C6 units-$^{15}$N2 lysine CNLM-291 or 4,4,5,5-D4 lysine CNLM-2640 0.0365 g/l) were added to produce "heavy" and "medium" SILAC medium, respectively.

**Endothelial cell growth medium.** Endothelial cell growth medium (ECGM) is low-glucose DMEM supplemented with 100 units/ml penicillin, 0.1 mg/ml streptomycin, 20 mmol/l HEPES, 1% nonessential amino acids, 50 mmol/l 2-mercaptoethanol, 20% heat-inactivated FCS, 12 units/ml heparin, and 150 μg/ml endothelial cell growth supplement (Sigma).

**Endothelial cell SILAC medium.** Endothelial cell SILAC medium is DMEM/K-/R- supplemented with 20 mmol/l HEPES, 1% nonessential amino acids, and 50 mmol/l 2-mercaptoethanol. SILAC isotopes were added as above.

**Preadipocyte growth medium.** Preadipocyte growth medium is DMEM/Ham's F-12 1:1 supplemented with 100 units/ml penicillin, 0.1 mg/ml streptomycin, and 10% FCS.

**Animals.** Male C57BL/6J mice were from Animal Resources Centre (Perth, Australia). Animals were kept in a temperature-controlled room (22 ± 1°C), 80% relative humidity, on a 12-h light/dark cycle with free access to food and water. Experiments were carried out with approval of Garvan Institute Animal Experimentation Ethics Committee, following guidelines issued by the National Health and Medical Research Council of Australia. For each experiment, 2–5 mice were used as tissue donors.

**Preparation of anti-CD31 (anti-PECAM-1) antibody-coated magnetic beads.** Sheep anti-rat IgG Dynabeads (Invitrogen) were precoated with rat anti-mouse monoclonal antibody to CD31 (PECAM-1) (BD Pharmingen) according to the manufacturer's instructions at a concentration of 1 μg antibody per $1 \times 10^7$ Dynabeads. Dynabeads were stored in PBS with 0.1% BSA at 4°C at $4 \times 10^8$ beads/ml.

**Adipose tissue explants.** Paired VAT (epididymal) and SAT (inguinal) depots were obtained from 6-week old C57BL/6J mice. Fat pads were immediately transported in warm transfer medium to a tissue culture hood, where they were placed in fresh transfer medium and minced into ~1 mm$^3$ pieces. Minced explants were rinsed in PBS and centrifuged at 250*g* to remove cell debris and erythrocytes. Adipose tissue explants (200 μl) were incubated in 1 ml SILAC medium. After 48 h of incubation at 37°C in 5% $CO_2$, conditioned medium was collected and centrifuged at 2,000*g* to pellet cell debris. Lectin affinity chromatography and subsequent mass spectrometry were performed.

**Preadipocyte and endothelial cell isolation and culture.** Preadipocytes and microvascular endothelial cells (MVECs) were isolated from the same biopsies. Paired VAT and SAT depots were obtained from 6-week-old C57BL/6J mice. Fat pads were immediately transported in warm transfer medium to a tissue culture hood, where they were placed in fresh transfer medium and minced into ~1 mm$^3$ pieces. Medium was removed and replaced with fresh transfer medium containing 1 mg/ml collagenase type I and incubated with gentle shaking at 37°C for 1 h. Adipose tissue to digest solution ratio was 4:1. Resulting material was filtered through 250 μm mesh, and adipocytes and free oil were separated from stromovascular components by centrifugation at 250*g* for 5 min at room temperature. The stromovascular pellet was resuspended, washed in PBS, and centrifuged at 250*g* for 5 min at room temperature. This washing step was repeated twice. The stromovascular pellet was resuspended and plated in 2% gelatin-coated 10 cm dishes in ECGM. This mixed cell population was cultured for 5–6 days at 37°C in 5% $CO_2$. Cells were detached using 0.25% trypsin containing 3.42 mmol/l EDTA and trypsin neutralized by addition of Hank's balanced salt solution containing 5% FCS (HBSS-FCS). The cell solution was centrifuged at 600*g* for 5 min at room temperature. The cell pellet was resuspended in 0.5 ml HBSS-FCS and incubated with 25 μl of anti-CD31 (anti-PECAM-1) coated dynabeads for 15 min at 4°C under constant rotation. The cell/bead suspension was brought to a total volume of 10 ml with HBSS-FCS and MVECs selected by magnet. Nonselected cells in the wash were transferred to a fresh tube. The wash and selection procedure was repeated five times. Selected cells were resuspended in ECGM and transferred to 2% gelatin-coated culture dishes. After 3–5 days, cells were routinely passaged and plated at equal density in ECGM. Nonselected cells in wash medium were centrifuged at 600*g* for 5 min at room temperature. The resultant pellet was resuspended in preadipocyte growth medium and plated at equal density in 10 cm culture dishes. MVECs and preadipocytes were grown until confluent. At confluence, medium was replaced with endothelial cell SILAC medium and SILAC medium, respectively. After 48 h, conditioned medium was collected and centrifuged at 2,000*g* to pellet cell debris. Lectin affinity chromatography and subsequent mass spectrometry were performed.

**Lectin affinity chromatography.** Conditioned media from paired visceral and subcutaneous depots were mixed in 1:1 ratio, and glycoprotein purification was performed as previously described (30). Briefly, $MnCl_2$ was added to conditioned media to a final concentration of 1 mmol/l. Samples were incubated overnight at 4°C under constant rotation with 50 μl/ml of 50% slurry of Concanavalin A Sepharose beads (GE Healthcare). Beads were washed extensively with ConA binding buffer (0.5 mol/l NaCl, 0.1 mol/l Tris, 1 mmol/l $MnCl_2$, and 1 mmol/l $CaCl_2$, pH 7.4). Proteins were eluted with 0.3 mol/l methyl-α-D-mannopyranoside, 0.5 mol/l NaCl, 0.1 mol/l Tris, 10 mmol/l EDTA, and 10 mmol/l EGTA, pH 7.4. Eluted proteins were precipitated using chloroform/methanol (31).

**Mass spectrometry.** Peptide extraction and mass spectrometry were as previously described (30,32) using a Waters Ultima tandem mass spectrometer. Mascot distiller software (Matrix Sciences) was used for data analysis. SwissProt database was used for protein identification, taxonomy restricted to *Mus musculus*, mass spectrometry tolerance set at 0.5 Da, and mass spectrometry/mass spectrometry tolerance set at 0.05 Da. A minimum ion score of 60 was chosen as the criterion for positive identification. "Heavy (U-$^{13}$C6 units-$^{15}$N4 arginine, U-$^{13}$C6 units-$^{15}$N2 lysine) to light (naturally occurring lysine and arginine)" (H/L) and "medium (U-$^{13}$C6 arginine, 4,4,5,5-D4 lysine) to light" (M/L) isotope ratios were used to determine relative abundance of proteins from visceral or subcutaneous samples, respectively. As visceral and subcutaneous samples are mixed, nonlabeled proteins form a "common denominator" that both isotopes are measured against (Fig. 1). Isotope ratios below 0.05 were discounted as "no label incorporation." Signal peptides were determined using SignalP 3.0 (33).

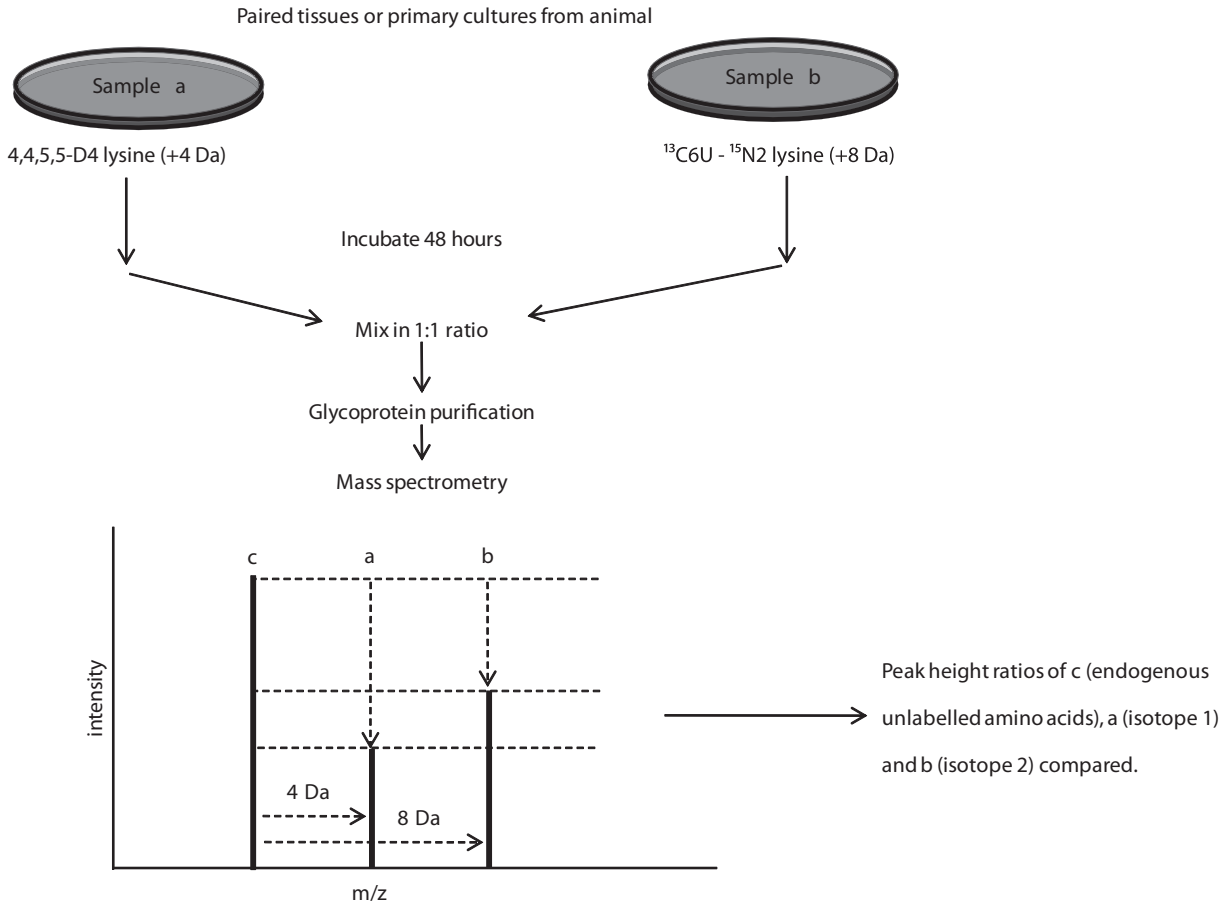


**FIG. 1. LAC–CILAIR workflow for comparing protein synthesis and secretion from two different samples. Paired cell cultures or tissues are incubated in media containing different isotopes of arginine and lysine, which are subsequently incorporated into newly synthesized and secreted proteins. Paired conditioned media samples are mixed in equal proportions, and proteins are subjected to mass spectrometry. Incorporation of amino acid isotopes results in a shift in molecular weight and mass to charge (*m/z*) ratio. Peak heights are measured, and their ratios are used to determine relative abundance of proteins from samples a and b.**

## RESULTS

We hypothesized there would be differences in protein secretion from VAT and SAT. Adipose tissue explants from epididymal (VAT) and inguinal (SAT) depots were incubated for 48 h in the presence of "heavy" and "medium" isotopes of arginine and lysine, respectively. Medium was collected, mixed in equal ratio, and subjected to LAC. Proteins were precipitated, resolved by SDS-PAGE, trypsin-digested, and subjected to quantitative mass spectrometry (Table 1 and supplementary data available in an online appendix at http://diabetes.diabetesjournals.org/cgi/content/full/db10-0483/DC1). A total of 145 proteins were identified, of which 86 (60%) were predicted to contain an $NH_2$-terminal signal peptide using SignalP. Of these, 51 proteins (59%) were present at >2-fold higher abundance in conditioned medium from VAT than SAT, whereas only 18 proteins (21%) were at >2-fold higher abundance in conditioned medium from SAT than VAT. The frequency distribution of the visceral-to-subcutaneous ratio for detected proteins is shown in Fig. 2*A*. Proteins without a signal peptide are nonspecifically released, newly synthesized cytosolic proteins. The distribution for these background proteins with no signal peptide resembles a normal distribution, whereas the distribution for proteins with a signal peptide is skewed to the right. This indicates that release of true secretory proteins into conditioned medium is increased from VAT relative to SAT. The normal distribution of nonsecretory background proteins indicates a similar amount of tissue was present in VAT and SAT samples.

Clustering analysis of detected proteins was performed using the database for annotation, visualization, and integrated discovery (DAVID) (34,35). Analysis of proteins increased from VAT revealed enrichment of proteins involved in endopeptidase inhibition, including members of the Serpin family, and proteins involved in innate immune system regulation, including members of the complement pathway. Cluster analysis of proteins increased from SAT showed no functional similarities.

Adipose tissue is composed of adipocytes as well as preadipocytes, MVECs, and macrophages, collectively referred to as the stromovascular fraction. Stromovascular cells may make a significant contribution to the secretory capacity of white adipose tissue, perhaps even exceeding that of adipocytes (36). Interplay between cells of the stromovascular fraction and adipocytes may also modulate the secretion profile of adipose tissue. We sought to determine the relative contribution of preadipocytes and MVECs to the whole adipose tissue secretome. In addition, we examined whether depot-specific differences in protein secretion observed from whole adipose tissue explants persisted in cells from the stromovascular fraction.

First we isolated preadipocytes from paired VAT and SAT biopsies. Visceral and subcutaneous preadipocytes

TABLE 1
Comparative secretion of proteins identified from visceral and subcutaneous white adipose tissue explants

| Description | Signal peptide? | Functional description | Accession |
|---|---|---|---|
| Complement C3 | + | Complement cascade, innate immunity | CO3_MOUSE |
| α-2-macroglobulin | + | Serine protease inhibitor, prevents coagulation and fibrinolysis | A2M_MOUSE |
| Laminin subunit β-1 | + | Extracellular matrix | LAMB1_MOUSE |
| Laminin subunit γ-1 | + | Extracellular matrix | LAMC1_MOUSE |
| Laminin subunit α-2 | + | Extracellular matrix | LAMA2_MOUSE |
| Collagen α-1(XIV) chain | + | Extracellular matrix | COEA1_MOUSE |
| Fibronectin | + | Extracellular matrix | FINC_MOUSE |
| Carboxylesterase 3 | + | Lipase | CES3_MOUSE |
| Haptoglobin | + | Haem binding protein, acute phase reactant | HPT_MOUSE |
| Collagen α-2(I) chain | + | Extracellular matrix | CO1A2_MOUSE |
| Serotransferrin | + | Iron binding | TRFE_MOUSE |
| Laminin subunit β-2 | + | Extracellular matrix | LAMB2_MOUSE |
| Complement factor B | + | Complement cascade, innate immunity | CFAB_MOUSE |
| Ceruloplasmin | + | Copper, iron binding | CERU_MOUSE |
| Serine protease inhibitor A3N | + | Trypsin inhibitor | SPA3N_MOUSE |
| Serine protease inhibitor A3K | + | Trypsin inhibitor, also known as contrapsin | SPA3K_MOUSE |
| Liver carboxylesterase N | + | Drug detoxification | ESTN_MOUSE |
| Gelsolin | + | Depolymerises extracellular actin from necrotic cells | GELS_MOUSE |
| Complement C4-B | + | Complement cascade, innate immunity | CO4B_MOUSE |
| Nidogen-2 | + | Extracellular matrix | NID2_MOUSE |
| Cathepsin B | + | Protease activity | CATB_MOUSE |
| Antithrombin-III | + | Serine protease inhibitor, regulation of blood coagulation | ANT3_MOUSE |
| Decorin | + | Extracellular matrix | PGS2_MOUSE |

Visceral or subcutaneous WAT explants were incubated in media containing different isotopes of arginine and lysine. Conditioned media were mixed, subjected to lectin affinity chromatography, and subjected to quantitative mass spectrometry. Peak height ratios of isotope to endogenous ($^{12}$C) amino acids and ratios between isotopes are shown. Complete dataset available in supplementary data.

were cultured in vitro for at least one week before incubation in medium containing isotopic amino acids. Conditioned medium was analyzed as before (Table 2 and supplementary data). Preadipocytes secreted a more limited set of proteins than minced adipose tissue. Of 23 proteins detected, 22 were secretory proteins. Of these, 15 were upregulated >2-fold from visceral compared with subcutaneous preadipocytes. Not one protein was upregulated >2-fold from subcutaneous as compared with visceral preadipocytes. The frequency distribution of the visceral-to-subcutaneous ratio for detected proteins is shown in Fig. 2*B* and is again skewed to the right. This indicates that the release of secretory proteins into conditioned medium is increased from visceral relative to subcutaneous preadipocytes. Cluster analysis of the proteins upregulated from visceral-derived preadipocytes showed an enrichment of extracellular matrix proteins.

Next, we examined MVECs isolated from paired VAT and SAT depots. To date the secretome of endothelial cells has not been determined. In addition, it is unknown whether MVECs display depot-specific differences. We isolated MVECs using CD31 magnetic bead separation and cultured these cells in vitro. Conditioned media from cells incubated in isotopic amino acids were collected and analyzed as before (Table 3 and supplementary data). Of 66 detected proteins, 34 (52%) displayed an $NH_2$-terminal signal peptide. Of these, 21 (62%) were increased >2-fold from visceral MVECs and only 5 were increased >2-fold from subcutaneous MVECs. The frequency distribution of the visceral to subcutaneous ratio for detected proteins is shown in Fig. 2*C*. Once again, these data are skewed toward increased protein secretion from visceral MVECs (Fig. 2*C*). This is consistent with the enhanced secretory capacity of VAT we have observed in both whole adipose tissue and isolated preadipocytes. The proteins identified include a number of proteins known to be secreted from endothelial cells, including thrombospondin-1 and thrombospondin-2, and extracellular matrix proteins such as fibronectin and collagens. Additionally, several proteins not previously known to be secreted from adipose tissue MVECs were identified. These include the most abundantly detected protein, adipocyte enhancer binding protein 1 (AEBP1). This protein influences inflammation in macrophages via a direct interaction with PXR and PPARγ sites. Multiple members of the complement pathway were also identified. Cluster analysis showed proteins more abundantly secreted from visceral MVECs were involved in extracellular matrix formation, including collagen and fibronectins, and endopeptidase inhibition, including members of the Serpin family. There were no defined clusters for the five secretory proteins more abundantly secreted from subcutaneous MVECs.

When the secretomes of whole adipose tissue explants, preadipocytes, and MVECs were compared, eight common secreted proteins were identified (Fig. 3). Seven secreted proteins were shared between the whole adipose tissue and MVEC secretomes, and four were shared between the whole adipose tissue and preadipocyte secretomes. These shared proteins included proteins involved in extracellular matrix formation, such as collagen and fibronectin, and other known adipocyte proteins known such as osteonectin. Interestingly, these data suggest the majority of proteins in the whole adipose tissue secretome are secreted either by adipocytes themselves or by other cells in the stromovascular fraction such as macrophages and neurons. To interrogate this further, we compared the secretome of whole adipose tissue explants to the secretomes of differentiated 3T3-L1 adipocytes (30) and isolated rat adipocytes

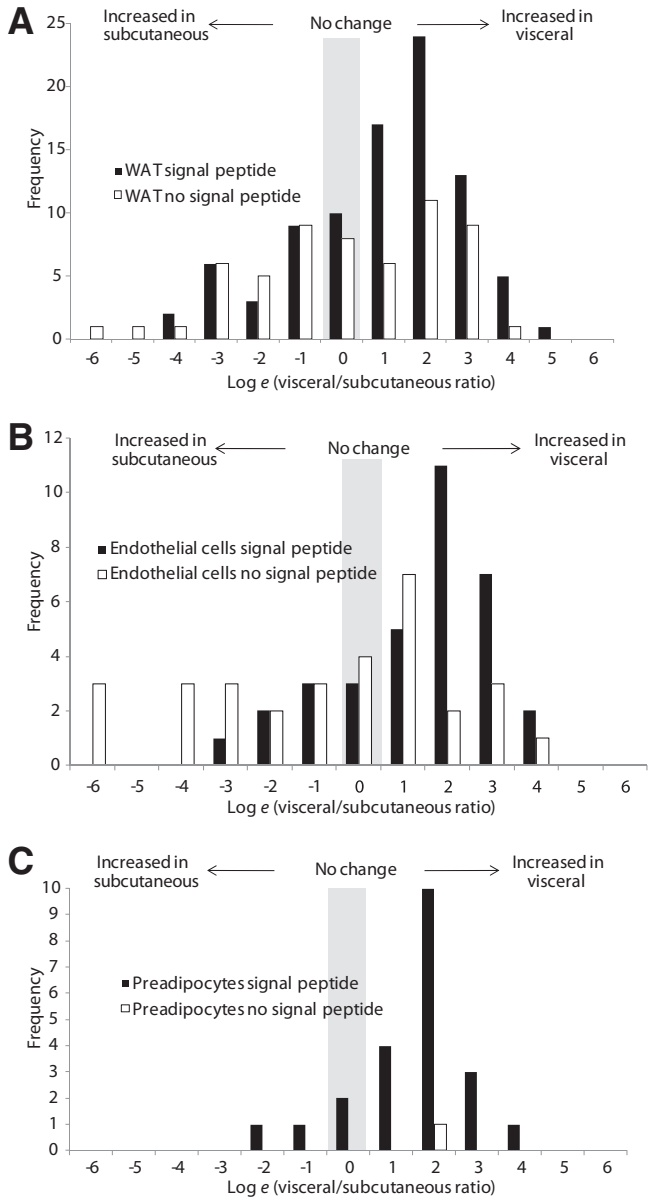


**FIG. 2.** ***A*****: White adipose tissue (WAT) explants secretory proteins are secreted in greater amounts from VAT.** ***B*****: Preadipocyte secreted proteins are secreted at greater amounts from visceral-derived preadipocytes.** ***C*****: Endothelial cell secretory proteins are secreted at greater amounts from visceral-derived endothelial cells. WAT explants, preadipocytes, and microvascular endothelial cells from visceral and subcutaneous WAT depots were cultured in media containing two different isotopes of arginine and lysine. LAC–CILAIR mass spectrometry was performed, and isotopic ratios were calculated. The histogram shows distribution of visceral-to-subcutaneous ratios for proteins detected. Note the use of the natural log scale.**

(27). Of the 86 proteins identified in the whole adipose tissue secretome, 26 were shared with the 3T3-L1 adipocyte secretome and 21 were shared with the isolated rat adipocyte secretome (Fig. 4). These data confirm that adipocytes alone are not the principal source of secreted proteins. It is possible that other cells types in the stromovascular fraction such as macrophages and neurons are the source of secreted proteins. To interrogate this further, we compared the secretome of whole adipose tissue explants to the secretome of human macrophages, and only three common proteins were identified (37).

## DISCUSSION

In this study, we have made three important observations. First, the overall secretory capacity of VAT is considerably higher than SAT, and second, this enhanced secretory capacity of VAT extends to cells of the stromovascular fraction—preadipocytes and MVECs. Third, adipose tissue as a whole secretes more proteins than its individual component parts, suggesting the adipocyte is not the principal secretory component of adipose tissue. The secretome of adipose tissue is likely due to the complex interplay between its component cell types.

To interrogate the adipose tissue secretome, we combined two techniques, CILAIR (29) and LAC (30). Using this streamlined method excluded contaminating proteins from entrapped serum and intracellular contents from damaged cells. Metabolic labeling identifies proteins that are newly synthesized during the culture period. Proteins already in the secretory pathway will remain unlabeled as will contaminants from serum and cell debris (38). LAC selectively enriches for proteins targeted for secretion, thus overcoming contamination from dead or damaged cells. Abundant serum proteins, such as albumin, that are nonglycosylated are removed. This obviates the need for multiple washing steps to dilute these contaminating serum proteins, decreasing sample processing time and the negative impact of prolonged tissue handing. Despite these measures, unlabeled proteins will remain in the medium. As conditioned media from visceral and subcutaneous samples are mixed, nonlabeled ("light") proteins form a "common denominator" that both isotopes are measured against. This eliminates any potential confounding from unlabeled contaminants differentially distributed between the two depots. The technique of LAC–CILAIR is a useful and valid tool for interrogation of the adipose tissue secretome, indicated by the detection of well-known adipokines including adiponectin, adipsin, and plasminogen activator inhibitor-1 (PAI-1).

First, we compared rates of protein secretion from VAT and SAT explants. VAT explants secreted quantitatively more proteins than SAT. Of proteins secreted in >2-fold abundance, 59% were from VAT explants compared with 21% from SAT explants. This upregulation of protein secretion from VAT was consistent across cells of the stromovascular fraction with 68% of proteins secreted in >2-fold abundance from VAT preadipocytes compared with 0% from SAT and 62% of proteins secreted in >2-fold abundance from VAT MVECs compared with 15% from SAT (Table 4). Preadipocytes and MVECs were cultured in vitro for at least one week prior to application of labeled media so were no longer subject to paracrine influences from their depot of origin. This suggests increased protein secretion is an intrinsic characteristic of components of VAT. The detection of a small number of proteins secreted in twofold greater abundance from subcutaneous depots provides evidence that our technique does not selectively detect enhanced protein secretion from the visceral depot.

Cluster analysis of proteins secreted in greater abundance from VAT revealed members of the acute phase response and innate immune system. These data raise two interesting hypotheses. The first is that VAT is more pro-angiogenic than SAT, as many members of the acute phase response, for example, haptoglobin (39), and innate immune system (40) are involved in angiogenesis. The capacity for angiogenesis is a crucial requirement for adipose tissue expansion, and cells of the adipose tissue

TABLE 2
Comparative secretion of proteins identified from visceral and subcutaneous adipose tissue–derived preadipocytes

| Description | Signal peptide? | Functional description | Accession |
|---|---|---|---|
| Collagen α-1(I) chain | + | Extracellular matrix | CO1A1_MOUSE |
| Collagen α-2(I) chain | + | Extracellular matrix | CO1A2_MOUSE |
| Collagen α-1(III) chain | + | Extracellular matrix | CO3A1_MOUSE |
| Collagen α-2(V) chain | + | Extracellular matrix | CO5A2_MOUSE |
| Fibronectin | + | Extracellular matrix | FINC_MOUSE |
| Fibulin-2 | + | Extracellular matrix | FBLN2_MOUSE |
| SPARC | + | Angiogenesis inhibitor | SPRC_MOUSE |
| Pigment epithelium-derived factor | + | Angiogenesis inhibitor, role in insulin resistance | PEDF_MOUSE |
| Collagen α-1(V) chain | + | Extracellular matrix | CO5A1_MOUSE |
| Haptoglobin | + | Haem binding protein, acute phase reactant | HPT_MOUSE |
| Cathepsin B | + | Protease activity | CATB_MOUSE |
| Plasma protease C1 inhibitor | + | Inhibits C1s and C1r protease activity | IC1_MOUSE |
| Plasminogen activator inhibitor 1 | + | Serine protease inhibitor, inhibits matrix metalloproteinases, associated with insulin resistance | PAI1_MOUSE |
| Collagen α-1(II) chain | + | Extracellular matrix | CO2A1_MOUSE |
| Metalloproteinase inhibitor 1 | + | Regulation of extracellular matrix | TIMP1_MOUSE |
| Collagen α-1(IV) chain | + | Extracellular matrix | CO4A1_MOUSE |
| Titin | - | Mechanical contraction | TITIN_MOUSE |
| Biglycan | + | Extracellular matrix | PGS1_MOUSE |
| Cathepsin L1 | + | Cysteine protease | CATL1_MOUSE |
| Epidermal growth factor receptor | + | Regulation of growth and proliferation | EGFR_MOUSE |
| Collagen α-2(XI) chain | + | Extracellular matrix | COBA2_MOUSE |
| Follistatin-related protein 1 | + | Growth factor binding | FSTL1_MOUSE |
| A disintegrin and metalloproteinase with thrombospondin motifs 7 | + | Regulation of extracellular matrix | ATS7_MOUSE |

Visceral or subcutaneous WAT-derived preadipocytes were incubated in media containing different isotopes of arginine and lysine. Conditioned media were mixed, subjected to lectin affinity chromatography, and subjected to quantitative mass spectrometry. Peak height ratios of isotope to endogenous ($^{12}$C) amino acids and ratios between isotopes are shown. Complete dataset available in supplementary data.

stromovascular fraction are able to differentiate into adipocytes and endothelial cells and vice versa (41). Anti-angiogenic agents have been proposed as novel therapeutic options in obesity as they induce weight loss in obese mouse models without adverse effect (42). In support of this hypothesis, cluster analysis of the 14

TABLE 3
Comparative secretion of proteins identified from visceral and subcutaneous adipose tissue–derived endothelial cells

| Description | Signal peptide? | Functional description | Accession |
|---|---|---|---|
| Tenascin | + | Extracellular matrix | TENA_MOUSE |
| Adipocyte enhancer-binding protein 1 | + | Transcriptional repressor | AEBP1_MOUSE |
| Collagen α-2(I) chain | + | Extracellular matrix | COL1A2_MOUSE |
| Thrombospondin-1 | + | Angiogenesis inhibitor | TSP1_MOUSE |
| Plasma protease C1 inhibitor | + | Inhibits C1s and C1r protease activity | IC1_MOUSE |
| EMILIN-1 | + | Extracellular matrix | EMIL1_MOUSE |
| Biglycan | + | Extracellular matrix | PGS1_MOUSE |
| Collagen α-1(I) chain | + | Extracellular matrix | CO1A1_MOUSE |
| Basement membrane-specific heparan sulfate proteoglycan core protein | + | Extracellular matrix | PGBM_MOUSE |
| Decorin | + | Extracellular matrix | PGS2_MOUSE |
| Collagen α-1(III) chain | + | Extracellular matrix | CO3A1_MOUSE |
| Plasminogen activator inhibitor 1 | + | Serine protease inhibitor, inhibits matrix metalloproteinases, associated with insulin resistance | PAI1_MOUSE |
| Titin | - | Mechanical contraction | TITIN_MOUSE |
| 14-3-3 protein ζ/δ | - | Phosphoprotein binding, modulation of enzymatic activity | 1433Z_MOUSE |
| α-2-macroglobulin | + | Serine protease inhibitor, prevents coagulation and fibrinolysis | A2M_MOUSE |
| Lipoprotein lipase | + | Lipoprotein associated lipid hydrolysis | LIPL_MOUSE |
| β-actin-like protein 2 | - | Cytoskeleton | ACTBL_MOUSE |
| Apolipoprotein E | + | Lipid transport | APOE_MOUSE |
| Inter-α-trypsin inhibitor heavy chain H3 | + | Serine protease inhibitor | ITIH3_MOUSE |
| Histone H2B type 1-C/E/G | - | DNA binding | H2B1C_MOUSE |

Visceral or subcutaneous WAT-derived endothelial cells were incubated in media containing different isotopes of arginine and lysine. Conditioned media were mixed, subjected to lectin affinity chromatography, and subjected to quantitative mass spectrometry. Peak height ratios of isotope to endogenous ($^{12}$C) amino acids and ratios between isotopes are shown. Complete dataset available in supplementary data.

TABLE 4
Summary of numbers of proteins detected and relative abundance between visceral and subcutaneous adipose tissue samples

| | WAT explants | Endothelial cells | Preadipocytes |
|---|---|---|---|
| Incorporated label | 145 | 66 | 23 |
| Signal peptide | 86 | 34 | 22 |
| Signal peptide, visceral/subcutaneous ratio > 2 | 51 | 21 | 15 |
| Signal peptide, subcutaneous/visceral ratio > 2 | 18 | 5 | 0 |
| No signal peptide, visceral/subcutaneous ratio > 2 | 23 | 10 | 1 |
| No signal peptide, subcutaneous/visceral ratio > 2 | 22 | 14 | 0 |
| % of proteins identified with signal peptide | 59 | 52 | 96 |
| % of total ion score from signal peptide containing proteins | 88 | 76 | 99 |

proteins secreted more abundantly from visceral preadipocytes revealed proteins involved in extracellular matrix production. This, together with our finding that VAT secretes pro-angiogenic factors, suggests that visceral preadipocytes are better adapted for rapid adipose tissue expansion than subcutaneous preadipocytes. The second hypothesis is that VAT secretes proinflammatory cytokines. This is consistent with recent data that VAT, particularly in obesity, develops chronic low-grade inflammation with macrophage infiltration. This is associated with insulin resistance. Proteins involved in macrophage recruitment were secreted in greater abundance from visceral MVECs. This suggests that adipose tissue MVECs play a pivotal role in enticing circulating macrophages into adipose tissue. However, adipose tissue used for this study was derived from young, lean animals. In this setting, the upregulation of these cytokines is more likely targeted for angiogenesis and adipose tissue proliferation rather than a proinflammatory milieu. Furthermore, recruitment of macrophages into adipose tissue is not always associated with inflammation as macrophages in adipose tissue from lean mice express IL-10, which protects adipocytes from insulin resistance (43).

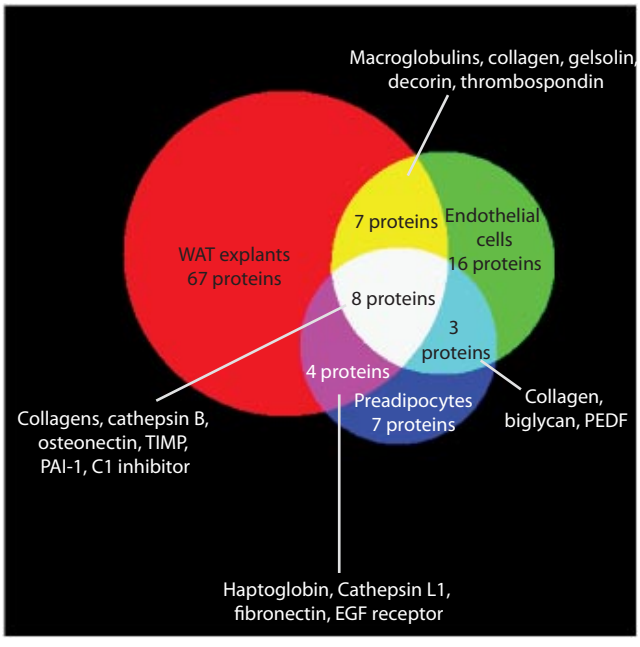


**FIG. 3. Venn diagram showing overlapping proteins detected from samples. A total of 116 secretory proteins were detected across all samples. PEDF, pigment epithelial derived factor; TIMP, tissue inhibitor of metalloproteinase 1. The diagram was composed using 3-Venn applet (48). (A high-quality color representation of this figure is available in the online issue.)**

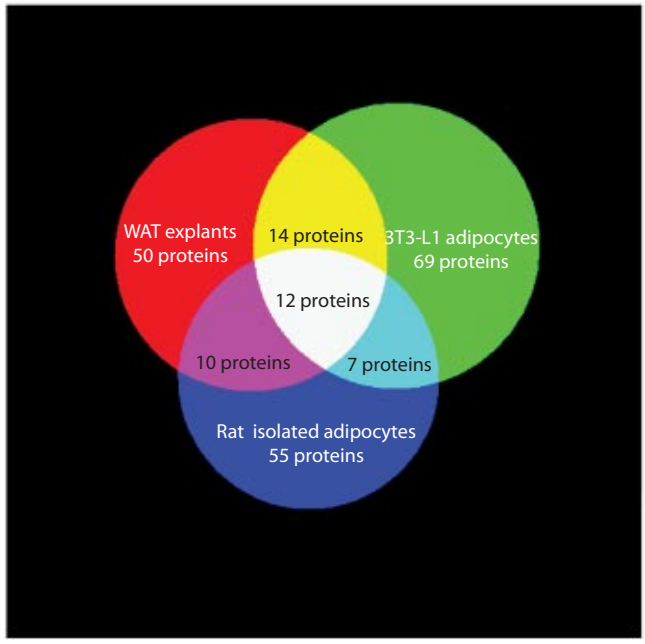


**FIG. 4. Venn diagram showing overlap of protein secretion from WAT explants, 3T3–L1 adipocytes, and isolated rat adipocytes (from ref 27). The 12 proteins detected in all three samples were adiponectin, adipsin, angiotensinogen (SerpinA8), cathepsin B, cathepsin D, collagen α-1(IV), collagen α-2(IV), complement C1s, haptoglobin, laminin subunit β-2, osteonectin, and thrombospondin-1. The diagram was composed using 3-Venn applet (48). (A high-quality color representation of this figure is available in the online issue.)**

This study represents the first survey of the endothelial cell secretome. In comparing MVECs from VAT and SAT, significant differences in protein secretion were demonstrated. Among the endothelial secretome were thrombospondins 1, 2, and 3, known to be secreted by endothelial cells, as well as a number of proteins not previously documented as endothelial secreted factors. Surprisingly, many were known adipocyte secretory proteins, including growth arrest specific 6, PAI-1, periostin, pentraxin-related protein 3, and SPARC. Of particular interest was identification of AEBP1, a secreted protein proposed to act as a transcriptional repression factor through binding of the enhancer sequence of the aP2/FABP4 gene in adipocytes, as well as PPARγ and LXR sites in macrophages (44,45) Preadipocytes deficient in AEBP1 are hyperproliferative, with enhanced adipogenesis (46). AEBP1 can be detected in whole adipose tissue samples, but not when adipocytes are purified from adipose tissue (47). Given our discovery of AEBP1 secretion from endothelial cells, we consider it likely that the source of AEBP1 in adipose tissue is endothelial cells. In this study, we found that MVECs from VAT secreted far more AEBP1

than MVECs from SAT. This observation could be important for explaining the deleterious effects of visceral adipose tissue.

In this study, we interrogated the secretome of whole adipose tissue and subsequently cells of the stromovascular fraction, preadipocytes and MVECs, to determine which component of adipose tissue was principally responsible for adipokine secretion. A total of 115 proteins were identified from these three samples, of which 67 were unique to adipose tissue explants, 16 were unique to MVECs, and 7 were unique to preadipocytes. Eight proteins were identified in all samples, including members of the collagen family, osteonectin, metalloproteinase inhibitor 1, C1 esterase inhibitor, plasminogen activator inhibitor-1, and cathepsin B. These data suggest adipocytes themselves or other cells in the stromovascular fraction not interrogated in this study, including macrophages and neurons, are the key secretory cells within adipose tissue. When the secretome of whole adipose tissue was compared with the secretomes of both differentiated 3T3-L1 adipocytes and primary rat adipocytes, only 26 (29%) and 20 (22%) common proteins, respectively, were identified. These data infer that adipocytes alone are not the principal source of secreted proteins in adipose tissue. As the adipose tissue came from lean animals, the expected number of macrophages should be low and in fact only three secreted proteins common to the secretomes of whole adipose tissue and human macrophages were found. This leads to the important conclusion that the secretome of whole adipose tissue is not simply the sum of each of its component parts but is the result of a paracrine interaction between the multiple cell types within adipose tissue.

## ACKNOWLEDGMENTS

This work was supported by grants from the National Health and Medical Research Council of Australia and Australian Postgraduate Awards. No potential conflicts of interest relevant to this article were reported.

L.W. designed experiments, researched data (mass spectrometry), analyzed data, and wrote the manuscript. S.H. designed experiments, researched data (isolation of fat pads, preadipocytes, endothelial cells), analyzed data, and wrote the manuscript. M.G. provided guidance for mass spectrometry experiments and was sadly deceased prior to project completion. D.J.C. reviewed/edited the manuscript. D.E.J. provided intellectual guidance, contributed to experimental design and discussion, and reviewed/edited the manuscript.

We thank Dr. Jerry Greenfield, the Garvan Institute of Medical Research and St Vincents' Hospital, and Dr. Shane Gray, the Garvan Institute of Medical Research, for reviewing the manuscript and the Biological Testing Facility, the Garvan Institute of Medical Research, for help with animal care.

## REFERENCES

1. Carey DG, Jenkins AB, Campbell LV, Freund J, Chisholm DJ. Abdominal fat and insulin resistance in normal and overweight women: Direct measurements reveal a strong relationship in subjects at both low and high risk of NIDDM. Diabetes 1996;45:633–638
2. Björntorp P. Abdominal obesity and risk. Clin Exp Hypertens A 1990;12:783–794
3. Kissebah AH, Vydelingum N, Murray R, Evans DJ, Hartz AJ, Kalkhoff RK, Adams PW. Relation of body fat distribution to metabolic complications of obesity. J Clin Endocrinol Metab 1982;54:254–260
4. Vague J. The degree of masculine differentiation of obesities: a factor determining predisposition to diabetes, atherosclerosis, gout, and uric calculous disease. Am J Clin Nutr 1956;4:20–34
5. Barzilai N, Banerjee S, Hawkins M, Chen W, Rossetti L. Caloric restriction reverses hepatic insulin resistance in aging rats by decreasing visceral fat. J Clin Invest 1998;101:1353–1361
6. Björntorp P. "Portal" adipose tissue as a generator of risk factors for cardiovascular disease and diabetes. Arteriosclerosis 1990;10:493–496
7. Nielsen S, Guo Z, Johnson CM, Hensrud DD, Jensen MD. Splanchnic lipolysis in human obesity. J Clin Invest 2004;113:1582–1588
8. Gabriely I, Ma XH, Yang XM, Atzmon G, Rajala MW, Berg AH, Scherer P, Rossetti L, Barzilai N. Removal of visceral fat prevents insulin resistance and glucose intolerance of aging: an adipokine-mediated process? Diabetes 2002;51:2951–2958
9. Abate N, Garg A, Peshock RM, Stray-Gundersen J, Grundy SM. Relationships of generalized and regional adiposity to insulin sensitivity in men. J Clin Invest 1995;96:88–98
10. Goodpaster BH, Thaete FL, Simoneau JA, Kelley DE. Subcutaneous abdominal fat and thigh muscle composition predict insulin sensitivity independently of visceral fat. Diabetes 1997;46:1579–1585
11. Engfeldt P, Arner P. Lipolysis in human adipocytes, effects of cell size, age and of regional differences. Horm Metab Res Suppl 1988;19:26–29
12. Wajchenberg BL. Subcutaneous and visceral adipose tissue: their relation to the metabolic syndrome. Endocr Rev 2000;21:697–738
13. Fried SK, Russell CD, Grauso NL, Brolin RE. Lipoprotein lipase regulation by insulin and glucocorticoid in subcutaneous and omental adipose tissues of obese women and men. J Clin Invest 1993;92:2191–2198
14. Rebuffé-Scrive M, Brönnegard M, Nilsson A, Eldh J, Gustafsson JA, Björntorp P. Steroid hormone receptors in human adipose tissues. J Clin Endocrinol Metab 1990;71:1215–1219
15. Gesta S, Blüher M, Yamamoto Y, Norris AW, Berndt J, Kralisch S, Boucher J, Lewis C, Kahn CR. Evidence for a role of developmental genes in the origin of obesity and body fat distribution. Proc Natl Acad Sci U S A 2006;103:6676–6681
16. Galic S, Oakhill JS, Steinberg GR. Adipose tissue as an endocrine organ. Mol Cell Endocrinol 2010;316:129–139
17. Van Harmelen V, Reynisdottir S, Eriksson P, Thörne A, Hoffstedt J, Lönnqvist F, Arner P. Leptin secretion from subcutaneous and visceral adipose tissue in women. Diabetes 1998;47:913–917
18. Lihn AS, Bruun JM, He G, Pedersen SB, Jensen PF, Richelsen B. Lower expression of adiponectin mRNA in visceral adipose tissue in lean and obese subjects. Mol Cell Endocrinol 2004;219:9–15
19. Klöting N, Graham TE, Berndt J, Kralisch S, Kovacs P, Wason CJ, Fasshauer M, Schön MR, Stumvoll M, Blüher M, Kahn BB. Serum retinol-binding protein is more highly expressed in visceral than in subcutaneous adipose tissue and is a marker of intra-abdominal fat mass. Cell Metab 2007;6:79–87
20. Bruun JM, Lihn AS, Pedersen SB, Richelsen B. Monocyte chemoattractant protein-1 release is higher in visceral than subcutaneous human adipose tissue (AT): implication of macrophages resident in the AT. J Clin Endocrinol Metab 2005;90:2282–2289
21. Bruun JM, Lihn AS, Madan AK, Pedersen SB, Schiøtt KM, Fain JN, Richelsen B. Higher production of IL-8 in visceral vs. subcutaneous adipose tissue. Implication of nonadipose cells in adipose tissue. Am J Physiol Endocrinol Metab 2004;286:E8–E13
22. Weisberg SP, McCann D, Desai M, Rosenbaum M, Leibel RL, Ferrante AW Jr. Obesity is associated with macrophage accumulation in adipose tissue. J Clin Invest 2003;112:1796–1808
23. Hotamisligil GS, Shargill NS, Spiegelman BM. Adipose expression of tumor necrosis factor-alpha: direct role in obesity-linked insulin resistance. Science 1993;259:87–91
24. Curat CA, Wegner V, Sengenès C, Miranville A, Tonus C, Busse R, Bouloumié A. Macrophages in human visceral adipose tissue: increased accumulation in obesity and a source of resistin and visfatin. Diabetologia 2006;49:744–747
25. Kratchmarova I, Kalume DE, Blagoev B, Scherer PE, Podtelejnikov AV, Molina H, Bickel PE, Andersen JS, Fernandez MM, Bunkenborg J, Roepstorff P, Kristiansen K, Lodish HF, Mann M, Pandey A. A proteomic approach for identification of secreted proteins during the differentiation of 3T3–L1 preadipocytes to adipocytes. Mol Cell Proteomics 2002;1:213–222
26. Wang P, Mariman E, Keijer J, Bouwman F, Noben JP, Robben J, Renes J. Profiling of the secreted proteins during 3T3–L1 adipocyte differentiation leads to the identification of novel adipokines. Cell Mol Life Sci 2004;61:2405–2417
27. Chen X, Cushman SW, Pannell LK, Hess S. Quantitative proteomic analysis

of the secretory proteins from rat adipose cells using a 2D liquid chromatography-MS/MS approach. J Proteome Res 2005;4:570–577
28. Zvonic S, Lefevre M, Kilroy G, Floyd ZE, DeLany JP, Kheterpal I, Gravois A, Dow R, White A, Wu X, Gimble JM. Secretome of primary cultures of human adipose-derived stem cells: modulation of serpins by adipogenesis. Mol Cell Proteomics 2007;6:18–28
29. Roelofsen H, Dijkstra M, Weening D, de Vries MP, Hoek A, Vonk RJ. Comparison of isotope-labeled amino acid incorporation rates (CILAIR) provides a quantitative method to study tissue secretomes. Mol Cell Proteomics 2009;8:316–324
30. Crowe S, Wu LE, Economou C, Turpin SM, Matzaris M, Hoehn KL, Hevener AL, James DE, Duh EJ, Watt MJ. Pigment epithelium-derived factor contributes to insulin resistance in obesity. Cell Metab 2009;10:40–47
31. Wessel D, Flügge UI. A method for the quantitative recovery of protein in dilute solution in the presence of detergents and lipids. Anal Biochem 1984;138:141–143
32. Larance M, Ramm G, Stöckli J, van Dam EM, Winata S, Wasinger V, Simpson F, Graham M, Junutula JR, Guilhaus M, James DE. Characterization of the role of the Rab GTPase-activating protein AS160 in insulin-regulated GLUT4 trafficking. J Biol Chem 2005;280:37803–37813
33. Bendtsen JD, Nielsen H, von Heijne G, Brunak S. Improved prediction of signal peptides: SignalP 3.0. J Mol Biol 2004;340:783–795
34. Dennis G Jr, Sherman BT, Hosack DA, Yang J, Gao W, Lane HC, Lempicki RA. DAVID: Database for Annotation, Visualization, and Integrated Discovery. Genome Biol 2003;4:P3
35. Huang da W, Sherman BT, Lempicki RA. Systematic and integrative analysis of large gene lists using DAVID bioinformatics resources. Nat Protoc 2009;4:44–57
36. Fain JN, Madan AK, Hiler ML, Cheema P, Bahouth SW. Comparison of the release of adipokines by adipose tissue, adipose tissue matrix, and adipocytes from visceral and subcutaneous abdominal adipose tissues of obese humans. Endocrinology 2004;145:2273–2282
37. Dupont A, Tokarski C, Dekeyzer O, Guihot AL, Amouyel P, Rolando C, Pinet F. Two-dimensional maps and databases of the human macrophage proteome and secretome. Proteomics 2004;4:1761–1778
38. Alvarez-Llamas G, Szalowska E, de Vries MP, Weening D, Landman K, Hoek A, Wolffenbuttel BH, Roelofsen H, Vonk RJ. Characterization of the human visceral adipose tissue secretome. Mol Cell Proteomics 2007;6:589–600
39. Cid MC, Grant DS, Hoffman GS, Auerbach R, Fauci AS, Kleinman HK. Identification of haptoglobin as an angiogenic factor in sera from patients with systemic vasculitis. J Clin Invest 1993;91:977–985
40. Rohrer B, Long Q, Coughlin B, Wilson RB, Huang Y, Qiao F, Tang PH, Kunchithapautham K, Gilkeson GS, Tomlinson S. A targeted inhibitor of the alternative complement pathway reduces angiogenesis in a mouse model of age-related macular degeneration. Invest Ophthalmol Vis Sci 2009;50:3056–3064
41. Wosnitza M, Hemmrich K, Groger A, Gräber S, Pallua N. Plasticity of human adipose stem cells to perform adipogenic and endothelial differentiation. Differentiation 2007;75:12–23
42. Rupnick MA, Panigrahy D, Zhang CY, Dallabrida SM, Lowell BB, Langer R, Folkman MJ. Adipose tissue mass can be regulated through the vasculature. Proc Natl Acad Sci U S A 2002;99:10730–10735
43. Lumeng CN, Bodzin JL, Saltiel AR. Obesity induces a phenotypic switch in adipose tissue macrophage polarization. J Clin Invest 2007;117:175–184
44. He GP, Muise A, Li AW, Ro HS. A eukaryotic transcriptional repressor with carboxypeptidase activity. Nature 1995;378:92–96
45. Majdalawieh A, Zhang L, Fuki IV, Rader DJ, Ro HS. Adipocyte enhancer-binding protein 1 is a potential novel atherogenic factor involved in macrophage cholesterol homeostasis and inflammation. Proc Natl Acad Sci U S A 2006;103:2346–2351
46. Ro HS, Zhang L, Majdalawieh A, Kim SW, Wu X, Lyons PJ, Webber C, Ma H, Reidy SP, Boudreau A, Miller JR, Mitchell P, McLeod RS. Adipocyte enhancer-binding protein 1 modulates adiposity and energy homeostasis. Obesity 2007;15:288–302
47. Ro HS, Kim SW, Wu D, Webber C, Nicholson TE. Gene structure and expression of the mouse adipocyte enhancer-binding protein. Gene 2001;280:123–133
48. Chow S, Rodgers P. Extended Abstract: Constructing Area-Proportional Venn and Euler Diagrams with Three Circles. In Euler Diagrams Workshop, Paris, 2005